Journal of Neural Transmission
https://doi.org/10.1007/s00702-026-03283-0

RESEARCH

Excitation/inhibition balance subtypes in autism and their genetic, neural, and clinical profiles

Vardan Arutiunian[1] · Catherine A. W. Sullivan[6] · Megha Santhosh[1] · Emily Neuhaus[1,2,3] · Heather Borland[1] · Raphael A. Bernier[2] · Susan Y. Bookheimer[4,5] · Mirella Dapretto[4,5] · Allison Jack[9] · Shafali Jeste[10] · James C. McPartland[7] · Adam Naples[7] · John D. Van Horn[11,12] · Kevin A. Pelphrey[13] · Sara Jane Webb[1,2,3] · Abha R. Gupta[6,7,8]

Received: 15 May 2026 / Accepted: 31 August 2026

Abstract
Excitation (E)/inhibition (I) imbalance is considered a key mechanism in Autism Spectrum Disorder (ASD). However, E/I imbalance can have different etiologies with increased E relative to I (E>I) and increased I relative to E (E<I). Both neural profiles can be associated with altered clinical phenotype, suggesting "bell"-shape brain-behavior relationships. We derived E/I balance measures from resting-state EEG in a large sex-balanced sample of youths with and without autism (N=310; 164 youths with ASD and 146 typically developing (TD) youths) to address group discriminative power of neural markers, their relation to social skills, and the potential to define different neural subtypes within the autistic group. We also conducted genome-wide copy number variant (CNV) and gene expression analyses to provide additional insight into distinct neural subtypes in autism. A high-density 128-channel electroencephalography (EEG) was used to register neural activity of participants, blood samples were collected from the ASD youths to obtain genomic DNA, and rich behavioral phenotyping was provided for each participant. The results revealed three subgroups within the autistic cohort with the presence of "typical" E/I, E>I, and E<I neural profiles. The two subgroups with E/I imbalance had altered clinical phenotypes. In addition, these subgroups had different genetic profiles, showing that genes within identified CNVs had distinct expression patterns with the evidence of more *prenatal* (E<I) vs. *postnatal* (E>I) gene expression. The study suggests that the proposed clustering approach has relevance for the identification of clinically meaningful neural and genetic subtypes within a heterogeneous autistic cohort.

Keywords Autism spectrum disorder · Excitation/inhibition imbalance neural subtypes · Genome-wide CNV analysis · Gene expression analysis · Pre- vs postnatal gene expression

Introduction

Autism Spectrum Disorder (ASD) is a highly heterogeneous neurodevelopmental condition that currently affects ~ 1 out of 31 children (Shaw et al. 2025). The core symptoms include difficulties with social interaction/communication and the presence of stereotyped/repetitive behaviors and restricted interests (American Psychiatric Association 2013). Often, individuals with ASD have co-occurring conditions, including language impairments (Arutiunian et al. 2024; Kjelgaard and Tager-Flusberg 2001), intellectual disability (Polyak et al. 2015), attention deficits (Matson et al. 2013), atypical response to sensory information (Bhaskaran et al. 2023) and single-gene mutations (Sztainberg and Zoghbi 2016). Recent studies in humans and animals combining molecular, genetic, electrophysiological, and neuroimaging approaches have proposed that the imbalance between neural excitation (E) and inhibition (I) is one of the main neurobiological factors contributing to the pathophysiology of ASD (Gatto and Broadie 2010; Levin and Nelson 2015; Rubenstein and Merzenich 2003; Sohal and Rubenstein 2019; Yizhar et al. 2011). However, the studies have

Sara Jane Webb and Abha R. Gupta have equal contribution.

Extended author information available on the last page of the article

shown that, due to the highly heterogeneous nature of the ASD population, there can be multiple neural and clinical profiles with respect to E/I imbalance (Antoine et al. 2019).

Studies addressing E/I imbalance in ASD have suggested that the aberrant interaction between glutamatergic (excitatory) and gamma-aminobutyric acidergic (GABAergic; inhibitory) neurotransmission at the cellular level causes a reduction in signal-to-noise ratio in key neural circuits (Sohal and Rubenstein 2019). This, in turn, may result in enhanced (as well as reduced) "noise" in the cortex, which impacts synaptic plasticity during development and results in less effective information processing (Contractor et al. 2021; Sohal and Rubenstein 2019; Tang et al. 2021). The E/I imbalance theory of ASD has also been supported by the recent identification of *de novo* variants in many autism-related genes involved in excitatory and inhibitory signaling (Gilman et al. 2011; Hollestein et al. 2023). Importantly, alterations in E/I balance can be varied, with evidence of increased E over I and increased I over E due to the circuits' increased excitatory or inhibitory states (Antoine et al. 2019; Chao et al. 2010; Delattre et al. 2013; Dickinson et al. 2016).

Resting-state and stimulus-induced gamma-band (30–150 Hz) neural activity in electro-/magnetoencephalography (EEG/MEG) is one of the most frequently reported non-invasive measures of E/I balance in the cortex (Buzsáki and Wang 2012). Cellular studies using optogenetic manipulations have shown that gamma oscillations are generated by GABAergic interneurons expressing calcium-binding protein parvalbumin (PV+ basket cells), and gamma activity plays a significant role in a variety of higher-order neuronal regulatory processes (Agetsuma et al. 2018; Bartos et al. 2007; Cardin et al. 2009; Carlén et al. 2012; Espinoza et al. 2018; Le Magueresse and Monyer 2013; Sohal et al. 2009). A number of findings have suggested that gamma power is altered in ASD (Gandal et al. 2010; Rojas and Wilson 2014), can be associated with the clinical phenotype (Webb et al. 2023), and has the potential to distinguish children with ASD from neurotypical children in the first year of life with high sensitivity and specificity (Gabard-Durnam et al. 2019).

However, most of the previous studies have addressed raw (or absolute) gamma power, which consists of periodic (oscillatory) and aperiodic (arrhythmic) components of a neural field that are associated with different neurobiological mechanisms (Levin et al. 2020). The parameterization of spectral power into periodic and aperiodic activity is a relatively new methodological approach that can shed light on which neural mechanism is altered (Donoghue et al. 2020; Ostlund et al. 2022; Wilkinson et al. 2024; Wilkinson and Nelson 2021). For example, several modeling studies in animals and neural tissue have demonstrated that the *aperiodic exponent*, rather than the power of gamma itself, reflects the E/I balance, and that exponent characteristics can indicate whether the neural circuit has increased E or increased I (Gao et al. 2017). By parameterizing the neural spectral power into two components, it is possible not only to assess "raw" gamma power as previously reported, but also its components, such as the aperiodic exponent and aperiodic-adjusted gamma power. This, in turn, allows exploration of specific neural mechanisms of ASD related to clinical profiles and symptom trajectory with the potential for subclassification based on neural markers, specificity of intervention target, and improving objective markers for clinical trials.

The goal of the present study was to investigate EEG-based E/I balance metrics derived from the parameterization algorithm (aperiodic exponent as a main measure of E/I balance, aperiodic-adjusted gamma power, and raw gamma power) for a large sex-balanced sample of participants with and without ASD using resting-state paradigm. First, we provided between-group comparisons in raw and parameterized spectral power to assess whether the difference in raw power is driven by the oscillatory component (periodic) or aperiodic exponent. We also addressed diagnostic discriminative power (ASD vs. typically developing controls, TD) of these measures, their sensitivity and specificity, and the relation to social functioning (as one of the core diagnostic criteria) in the clinical group. Second, we hypothesized different neural profiles in the ASD group with respect to E/I imbalance, i.e., more E over I and more I over E in comparison to TD youth and a possible "bell"-shape clinical profile, such that both increased inhibition and increased excitation can be related to lower social skills. To identify different neural profiles within the ASD group, we applied a cluster-based analysis to the ASD group based on the E/I balance primary measure and behavioral/clinical social skills. The cluster analysis aimed to identify clinically meaningful neural subtypes within the ASD group to account for the highly heterogeneous nature of this neurodevelopmental disorder and to explore similarities and differences in clinical profiles between subgroups. Finally, we conducted genome-wide copy number variant (CNV) and gene expression analyses to evaluate whether genetics can provide additional insight into potential brain-behavior relationships in ASD and explain different neural subtypes within the ASD group.

Methods

Participants

A total of 310 English-speaking youth aged 8 to 17 years with valid EEG data were included in the study: 164 youth with

ASD (72 female, 92 male) and 146 TD youth (68 female, 78 male). Exclusion criteria were twin status, presence of known chromosomal abnormalities/single-gene conditions related to ASD (e.g., Rett syndrome, Fragile X Syndrome), co-occurring neurological disorders (e.g., epilepsy), significant visual and auditory impairments, or sensory-motor difficulties that would prevent completion of study procedures.

Data were collected from four sites and participants were recruited using flyers and recruitment lists using strategies that reflected best practices at each site.

Ethical oversight

The study was approved by the ethical oversight at each site as well as a centralized IRB. All procedures performed were in accordance with the ethical standards of the 1964 Helsinki declaration and its later amendments or comparable ethical standards. Informed consent was obtained from all parents of children participating in the study; children provided written assent.

Clinical and behavioral measures

All youth with ASD had a clinical diagnosis based on the DSM-4–TR or DSM-5 (American Psychiatric Association 2000, 2013) and met criteria on the Autism Diagnosis Observation Schedule – Second Edition (Lord et al. 2012), Autism Diagnostic Interview – Revised (Rutter et al. 2003b), caregiver-reported developmental history, and expert clinical judgment. All participants had either verbal or nonverbal IQ≥70 based on the Differential Ability Scales – Second Edition (DAS-II) School Aged Cognitive Battery (Elliott 2007). TD youth had no first- or second-degree family members with ASD and no elevation of ASD traits according to parent report on the Social Responsiveness Scale – Second Edition (SRS-2) (Constantino 2012) (T-score < 60) or the Social Communication Questionnaire (Rutter et al. 2003a) (raw score < 11). Adaptive skills were measured with the Vineland Adaptive Behavior Scales – Second Edition (VABS-2) standard scores (SS) in communication, socialization, and daily living skills domains with higher scores reflecting better adaptive skills (Sparrow et al. 2005). See Supplementary Table 1 for demographics, descriptive statistics, and measures characterization.

Electrophysiological analysis

EEG data acquisition

EEG data were collected with EGI 128-channel Net Amps 300 system with HydroCel nets (Magstim EGI Inc., Eugene OR), using Net Station 4.4.2, 4.5.1, or 4.5.2 with a standard Net Station acquisition template. Nets were available without outriders (eye electrodes 125, 126, 127, and 128) for participants with facial sensory sensitivities. The participant's behavior was monitored in real time during EEG collection. Data were collected at 500 Hz sampling rate, referenced to Cz electrode (vertex), and impedances were < 50 kΩ.

Resting-state EEG was acquired via an eyes open (EO) condition, and all participants were given the instruction: "You are going to watch short movies and then rest your eyes". The recording session consisted of three runs of 6 × 16-second blocks of videos (dynamic screen saver type images that had limited or slow movement). The videos were displayed at a height of 7–8.5 cm × 9.4–10.6 cm and resulting in a visual angle of 5.5–6.7° to 7.5–8.5°. The videos were small to reduce eye movements.

EEG data pre-processing

To calculate power spectral density (PSD), we used the Batch EEG Automated Processing Platform, BEAPP (Levin et al. 2018) in MATLAB 2021a, consisting of: (1) format the MFF file for Matlab; (2) band-pass filter 1–100 Hz; (3) downsampling from 500 Hz to 250 Hz; (4) implementation of the Harvard Automated Preprocessing Pipeline for EEG (HAPPE) module for artifact detection and rejection (Gabard-Durnam et al. 2018), including removal of 60 Hz line noise, rejection of bad channels, wavelet enhanced thresholding, Independent Component Analysis (ICA) with automated component rejection, bad channel interpolation, and re-referencing to average; (5) segmentation of the continuous file into 1 s epochs; (6) rejection of bad segments (± 40 μV); (7) calculation of the PSD using Hanning window on clean segments. A total of 15 electrodes over the frontal region were used for the analysis (electrodes # 23, F3-24, 27, 28, 20, 5, Fz-11, 12, 16, 6, 3, 117, 123, F4-124, 118). We used only the frontal region because previous studies showed that frontal electrodes better distinguished groups (ASD vs. TD) and were related to behavioral/clinical measures in the ASD group (Gabard-Durnam et al. 2019). PSD was calculated for each electrode and averaged within this region of interest.

EEG E/I balance metrics calculation

To model the periodic and aperiodic components of PSD (Donoghue et al. 2020), we used the *specparam* toolbox (Ostlund et al. 2022) in Python v3.10 with the following settings: *peak_width_limit* = [1.5, 6], *n_peaks* = 6, *peak_height* = 0.10, *peak_threshold* = 2, and *frequency_range* = [1,55]. For each participant, the model provided two parameters (aperiodic offset and aperiodic exponent) to describe the aperiodic 1/f signal. To determine an aperiodic-adjusted

gamma power, the aperiodic signal from the model was subtracted from the raw power spectrum, resulting in a flattened spectrum. For the statistical analysis, raw and aperiodic-adjusted power was calculated for the gamma frequency range (30–55 Hz) with the natural logarithmic transformation, whereas aperiodic exponent was calculated for the whole frequency range (1–55 Hz), see (Ostlund et al. 2022). We focused on the low gamma frequency band (30–55 Hz) to avoid potential effects of 60 Hz line noise and the notch filter.

ASD and TD groups did not differ in the number of artifact-free epochs: *ASD*, M_{epoch}= 101.06, range 62–123; *TD*, M_{epoch} = 101.85, range 78–123, $t(303.18) = -0.47$, $p = 0.63$.

Genetic analysis

Genome-wide genotyping

Blood samples were collected from the ASD participants ($N = 133$) to obtain genomic DNA and were processed by the Rutgers University Cell and Data Repository (RUCDR) or using standard protocols (Gentra Puregene Blood DNA extraction kit; Qiagen). Individuals were genotyped using the HumanOmni2.5 M-8 BeadChip microarray (Illumina). All DNA samples were hybridized and scanned on the Illumina iScan to minimize batch effects and variation. All participants had a genotyping call rate > 95%. Genotyping data were analyzed by PLINK v1.07 (Purcell et al. 2007) using the forward strand and confirmed the reported sex of all participants.

Copy number variant (CNV) detection

CNV detection (duplications and deletions) was performed using three algorithms: PennCNV v1.0.4, QuantiSNP v1.1, and GNOSIS (Sanders et al. 2011). Analysis and merging of CNV predictions used CNVision (Sanders et al. 2011). All rare genic CNVs (≥50% of CNV at ≤1% frequency in the Database of Genomic Variants (Sanders et al. 2011); hereafter, CNVs) predicted by at least PennCNV and QuantiSNP and having a CNVision pCNV of ≤0.001, that is, those considered high-quality predictions (Sanders et al. 2015), were obtained for further analysis. Subsequent analyses combined duplications and deletions to maximize the number of CNVs available for examination; separating the two types led to low numbers and statistical power. Rare genic CNVs were identified in 98 youth with ASD; outliers (based on standard quartiles calculation in boxplots, $N = 12$) were excluded from the further statistical analysis.

Gene expression levels

Gene-level human brain gene expression data (Platform GPL5175, Affymetrix GeneChip Human Exon 1.0 ST Array) generated as part of the BrainSpan project (hbatlas.org) (Kang et al. 2011) were downloaded from the NCBI GEO database (accession number GSE25219) as log2-transformed signal intensity values. Values ≥ 6 in at least one sample in one brain region are considered positive brain gene expression (Kang et al. 2011). Affymetrix ("Affymetrix. Exon Array Background Correction," 2005) uses background probes with matching guanine-cytosine content for background correction for all array probes.

Candidate gene lists from CNVs

Gene lists for the ASD subgroups were compiled from genes within CNVs identified in our participants. The lists were compared to look for overlapping genes, which were removed to create unique gene lists for each subgroup. We narrowed down our list of genes to those with positive expression in the brain.

Gene co-expression matrices

A gene co-expression matrix for each ASD subgroup was constructed using the mean expression value for each gene in each brain region for each brain sample for time periods of interest, i.e., from early development (10 postconceptional weeks, PCW) to 2 years (Kang et al. 2011), and calculating the Pearson correlation coefficient for each pairwise gene combination across all data points. Two genes were considered co-expressed if they had an absolute correlation coefficient $r \geq 0.7$.

Gene co-expression analysis

For the candidate genes from each ASD subgroup, the gene co-expression matrices were used to calculate the average degree (number of correlated gene-pair connections with an absolute correlation coefficient $r \geq 0.7$ divided by the number of genes involved in those connections) as well as the mean coefficient value (mean of the correlation coefficients $r \geq 0.7$). To visualize the gene co-expression network, edges were drawn between two genes if their absolute correlation coefficient $r \geq 0.7$, using the organic layout function in Cytoscape (Cline et al. 2007). Positive correlations are shown in blue, and negative correlations are shown in red ($r \geq 0.7$ in blue and $r \leq -0.7$ in red). The greater the magnitude of the coefficient, the wider the edges. The size of a node is proportional to the number of edges the node has (see Fig. 3E further).

Permutation testing

To compare the matrices for the different ASD subgroups, permutation testing with 10,000 iterations was performed by selecting the same number of genes found within the group with the original matrix to determine the significance of the average degree and mean coefficient value. We then compared the selected gene average degree, mean coefficient value, and the combination of both to the random selection of the same number of genes. The *p*-value was calculated by the number of iterations that resulted in a greater or equal average degree, mean coefficient value, and combination of both.

Median expression over lifetime

The median expression value for genes found to be correlated ($r \geq 0.7$ in time periods from 10 PCW to 2 years) in the ASD subgroups across all brain samples was determined and plotted in R (Core Team 2023) using *ggplot2* (Wickham 2016) for each brain region (NCX = neocortex, AMY = amygdala, MD = mediodorsal nucleus of the thalamus, HIP = hippocampus, STR = striatum, CBC = cerebellar cortex) and time period. Local polynomial regression fitting was used to smooth the scatter plots.

Table 1 Group discriminations with EEG E/I balance metrics (all *p*-values are FDR-corrected). Significant *p*-values are highlighted in bold

Models/Parameters	B coefficient	SE	z	*p*
Model 1 (ASD vs. TD)				
Raw gamma power	1.53	0.69	2.22	**0.04**
Age	–0.00	0.00	–0.64	0.52
Sex	0.18	0.23	0.78	0.52
Model 2 (ASD vs. TD)				
Aperiodic-adjusted gamma power	2.65	6.00	0.44	0.66
Age	–0.00	0.00	–1.47	0.18
Sex	0.15	0.23	0.65	0.52
Model 3 (ASD vs. TD)				
Aperiodic exponent	–3.30	1.27	–2.59	**0.03**
Age	–0.01	0.00	–2.30	0.07
Sex	0.21	0.23	0.90	0.52
Model 4 (ASD subgroup 1 vs. TD)				
Aperiodic exponent	–2.96	1.89	–1.57	0.12
Age	–0.01	0.00	–2.87	**0.01**
Sex	0.17	0.34	0.49	0.62
Model 5 (ASD subgroup 2 vs. TD)				
Aperiodic exponent	5.34	1.96	2.72	**0.009**
Age	–0.00	0.00	–1.05	0.45
Sex	0.35	0.32	1.08	0.62
Model 6 (ASD subgroup 3 vs. TD)				
Aperiodic exponent	–15.43	2.82	–5.47	**<0.001**
Age	–0.00	0.00	–0.71	0.48
Sex	0.25	0.40	0.62	0.62

Statistical analysis

Statistical analysis was performed in R (Core Team 2023). All linear models used in the analysis were estimated with the *lme4* package (Bates et al. 2015), effect sizes were calculated with the *effectsize* package (Ben-Shachar et al. 2020), and the data were plotted with *ggplot2* (Wickham 2016). The structure of the models will be specified further in the Results section. The figures, representing neural responses, were created with python data visualization library *matplotlib* (Hunter, 2007).

We applied the *k*-means clustering method to identify subgroups within the ASD group based on the EEG aperiodic exponent and VABS Socialization Standard Score. Prior to clustering, both variables were *z*-score standardized to ensure comparable scaling and equal contribution to the clustering procedure. The optimal number of clusters was evaluated using the *elbow method* based on the total within-cluster sum of squares. Visual inspection of the elbow plot supported a three-cluster solution. To reduce sensitivity to random centroid initialization, the *k*-means algorithm was run with 100 random starting configurations (*nstart* = 100), and the solution with the lowest total within-cluster sum of squares was retained. The resulting clusters were subsequently compared with the TD group in all downstream analyses. The cluster-based analysis was conducted using *factoextra* package (Kassambara and Mundt 2020). Cluster stability was assessed using bootstrap resampling using the *fpc* package in R (Hennig 2026). The three-cluster solution was evaluated across 1,000 bootstrap resampling iterations, and stability was quantified using the clusterwise Jaccard similarity coefficient, which measures the agreement between the original clustering solution and the corresponding clusters identified in the bootstrap samples.

For the receiver operating characteristic (ROC) curve analysis we, used the *pROC* package (Robin et al. 2011). A correction for multiple comparisons (false discovery rate, FDR) was applied to each set of the analyses, and *p*-values were corrected with the *p.adjust.method* in R.

Results

Between-group differences in excitation (E)/inhibition (I) balance measures

In order to determine whether EEG measures of E/I balance differentiate the ASD group from the TD controls, a set of logistic regression models were fitted (see Table 1, Models 1–3). The models predicted groups (ASD vs. TD) using EEG metrics (raw gamma power, aperiodic-adjusted gamma power, and aperiodic exponent, see Fig. 1A), and

accounting for age and sex. The results showed a statistically significant difference in raw gamma power with the evidence of higher power in the ASD group, β = 1.53, SE = 0.69, $z = 2.22$, $p = 0.04$; and in the aperiodic exponent, with lower slope values in the ASD group, β = −3.30, SE = 1.27, $z = -2.59$, $p = 0.03$ (Fig. 1B). These between-group differences in the EEG metrics suggested increased E over I in the neural networks in the ASD group.

To reveal the classification power of EEG metrics and to calculate their sensitivity and specificity, we applied ROC-curve analysis and calculated the area under the curves (AUCs) for three classification models. AUC, which reflects the percentage of correctly classified youth, for

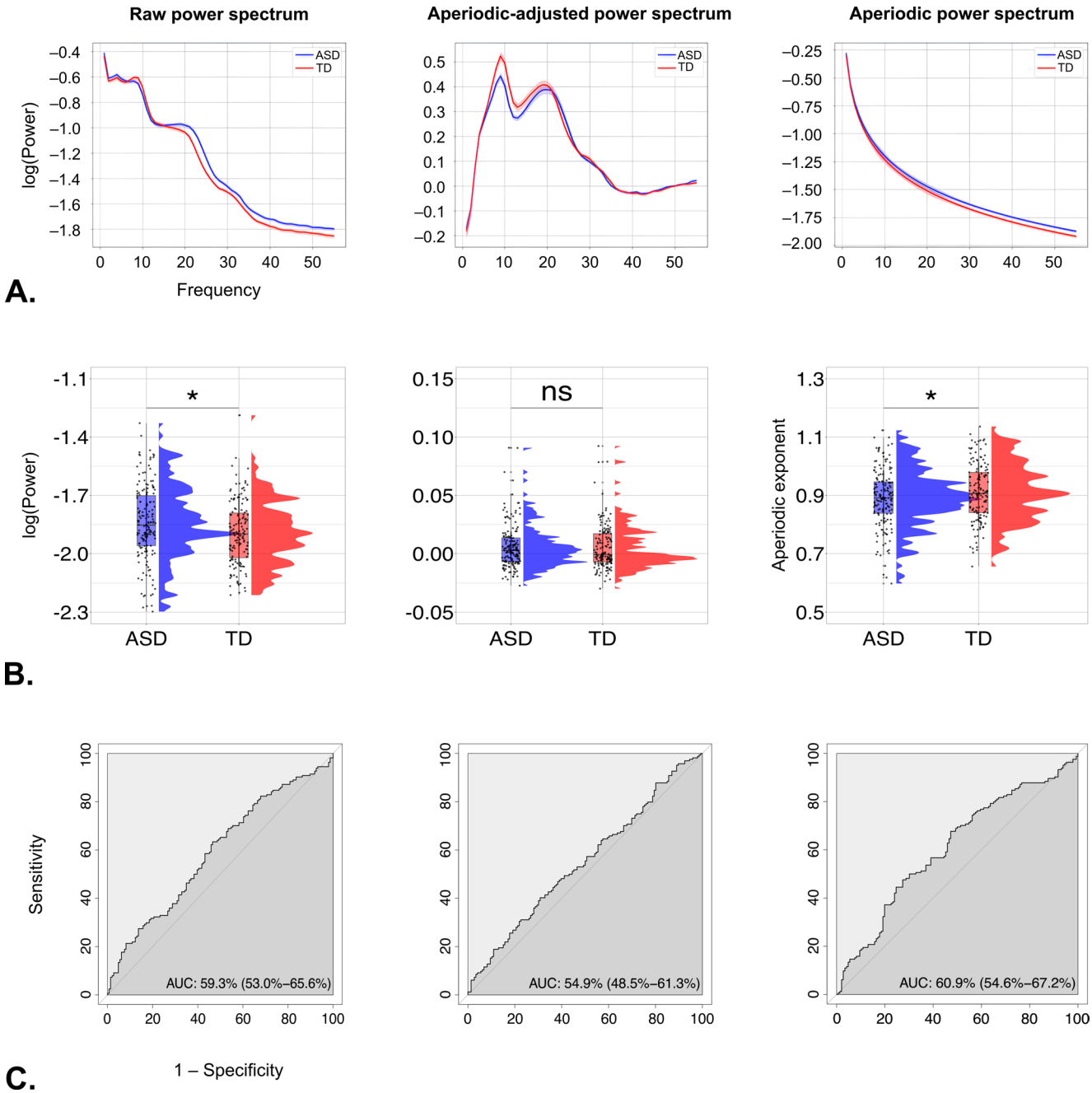

Fig. 1 Between-group comparisons (ASD = Autism Spectrum Disorder, TD = typically developing) in E/I balance metrics: (**A**) Raw power spectrum, aperiodic and periodic components of the spectrum; (**B**) Boxplots representing between-group differences for raw gamma power (left), aperiodic-adjusted gamma power (center), and aperiodic exponent (right); (**C**) Receiver operating characteristics curves for the classification models (ASD vs. TD) for raw gamma power (left), aperiodic-adjusted gamma power (medium), and aperiodic exponent (right), AUC = area under the curve. Significance is labeled with *$p < 0.05$, **$p < 0.01$, ns = non-significant. All p-values are FDR-corrected

Model 3 (with aperiodic exponent as the EEG variable) had the highest value (Table 2, Models 1–3). However, for all three EEG measures, classification accuracy was low (Fig. 1C): for Model 3 (aperiodic exponent) AUC-value was ***poor*** ($0.6 \leq AUC < 0.7$), whereas for Models 1 (raw gamma power) and 2 (aperiodic-adjusted gamma power) classification ***failed*** ($0.5 \leq AUC < 0.6$), see (Nahm 2022).

To assess whether E/I balance metrics were related to social skills of autistic youth, we fitted a linear model with the VABS Socialization SS as a dependent variable and three predictors (raw gamma power, aperiodic-adjusted gamma power, and aperiodic exponent) as main effects in the ASD group. The results showed that the aperiodic exponent predicted social skills, so that higher slope value (and, thus, less cortical excitability) was associated with higher socialization score, $\beta = 25.62$, $SE = 10.79$, $z = 2.37$, $p = 0.02$. Raw gamma power ($\beta = 3.54$, $SE = 5.55$, $z = 0.64$, $p = 0.52$) and aperiodic-adjusted gamma power ($\beta = 50.25$, $SE = 49.24$, $z = 1.02$, $p = 0.31$) were not related.

To summarize, the ASD group showed an elevated E over I neural pattern, and this increased excitatory activity was associated with lower social skills. As there was no between-group difference in aperiodic-adjusted gamma power, it is most likely that the between-group difference in raw gamma power was driven by the aperiodic component of PSD (raw gamma power and aperiodic exponent were highly correlated, $r = -0.44$, $p < 0.001$). Therefore, subsequent analysis focused only on this primary measure of E/I balance (i.e., aperiodic exponent).

Table 2 Model performance metrics discriminating autism groups

Models	Area under the curve (95% C.I.)	Sensitivity	Specificity
Model 1 (raw gamma power)			
ASD vs. TD	59.3% (53.0% – 65.6%)	53.4%	63.4%
Model 2 (aperiodic-adjusted gamma power)			
ASD vs. TD	54.9% (48.5%–61.3%)	69.2%	40.2%
Model 3 (aperiodic exponent)			
ASD vs. TD	60.9% (54.6% – 67.2%)	52.7%	67.7%
Model 4 (aperiodic exponent)			
ASD subgroup 1 vs. TD	63.5% (54.0% – 73.1%)	65.8%	64.8%
Model 5 (aperiodic exponent)			
ASD subgroup 2 vs. TD	65.1% (57.7% – 72.4%)	36.3%	96.8%
Model 6 (aperiodic exponent)			
ASD subgroup 3 vs. TD	82.8% (76.6% – 88.9%)	64.4%	93.6%

Area under the curve (AUC) represents a percentage of correctly classified youth ($90\% \leq AUC$, *excellent*; $80\% \leq AUC < 90\%$, *good*; $70\% \leq AUC < 80\%$, *fair*; $60\% \leq AUC < 70\%$, *poor*; $50\% \leq AUC < 60\%$, *fail*; see (61)).

Age-related changes in E/I balance

The previous findings showed age-related changes in the aperiodic signal, with the evidence that the slope value decreased with age (Ostlund et al. 2022). To test this, we conducted Pearson's correlation of aperiodic exponent and age within each diagnostic group. Although we found between-group differences in aperiodic exponent, the results indicated similar age-related pattern in both groups, *TD group*, $r = -0.40$, $p < 0.001$; *ASD group*, $r = -0.33$, $p < 0.001$. This suggested that a lower exponent was associated with higher age, confirming the previous findings (Fig. 2A). Visual examination of the mean trajectory showed that the decline in exponent started after 12.5 years of age in both groups.

Subgrouping the ASD sample based on aperiodic exponent and social skills

Given the possibility of different neural profiles with respect to E/I balance in the ASD group (both E < I and E > I) as well as "bell"-shape relationships between E/I balance metrics and clinical characteristics (both pathological increase and decrease of E/I balance can be associated with lower social skills), we conducted a cluster-based analysis in the ASD group using the aperiodic exponent and VABS Socialization SS. Four participants were excluded from this analysis, as VABS Socialization SS was not available for them, resulting in 160 individuals with ASD. The *elbow method* of cluster number selection revealed that the optimal number of clusters was *three* and divided the ASD group into three subgroups/clusters (Fig. 2B), consisting of 50 (23 female), 63 (24 female), and 47 (24 female) participants. Bootstrap analysis indicated moderate stability of the three-cluster solution. The mean clusterwise Jaccard similarity coefficients were 0.707, 0.714, and 0.682 for clusters 1, 2, and 3, respectively, indicating moderate reproducibility of the clustering solution across 1,000 bootstrap resampling iterations.

To assess whether aperiodic exponent discriminates ASD subgroups from the TD group, three logistic regression models were fitted (see Table 1, Models 4–6). The models predicted groups (ASD subgroup vs. TD) using EEG E/I balance metric (aperiodic exponent) accounting for age and sex. The results showed no difference between the TD group and the ASD subgroup 1 (ASD_1), $\beta = -2.96$, $SE = 1.89$, $z = -1.57$, $p = 0.12$. However, there was a significant difference between the TD group and the other two ASD subgroups, and the directions of the effects were opposite (Fig. 2C). The aperiodic exponent was higher in the ASD subgroup 2 (ASD_2) when compared to the TD group, showing E < I neural profile (i.e., more inhibition), $\beta = 5.34$, $SE = 1.96$, $z = 2.72$, $p = 0.009$. In contrast, the ASD subgroup 3 (ASD_3)

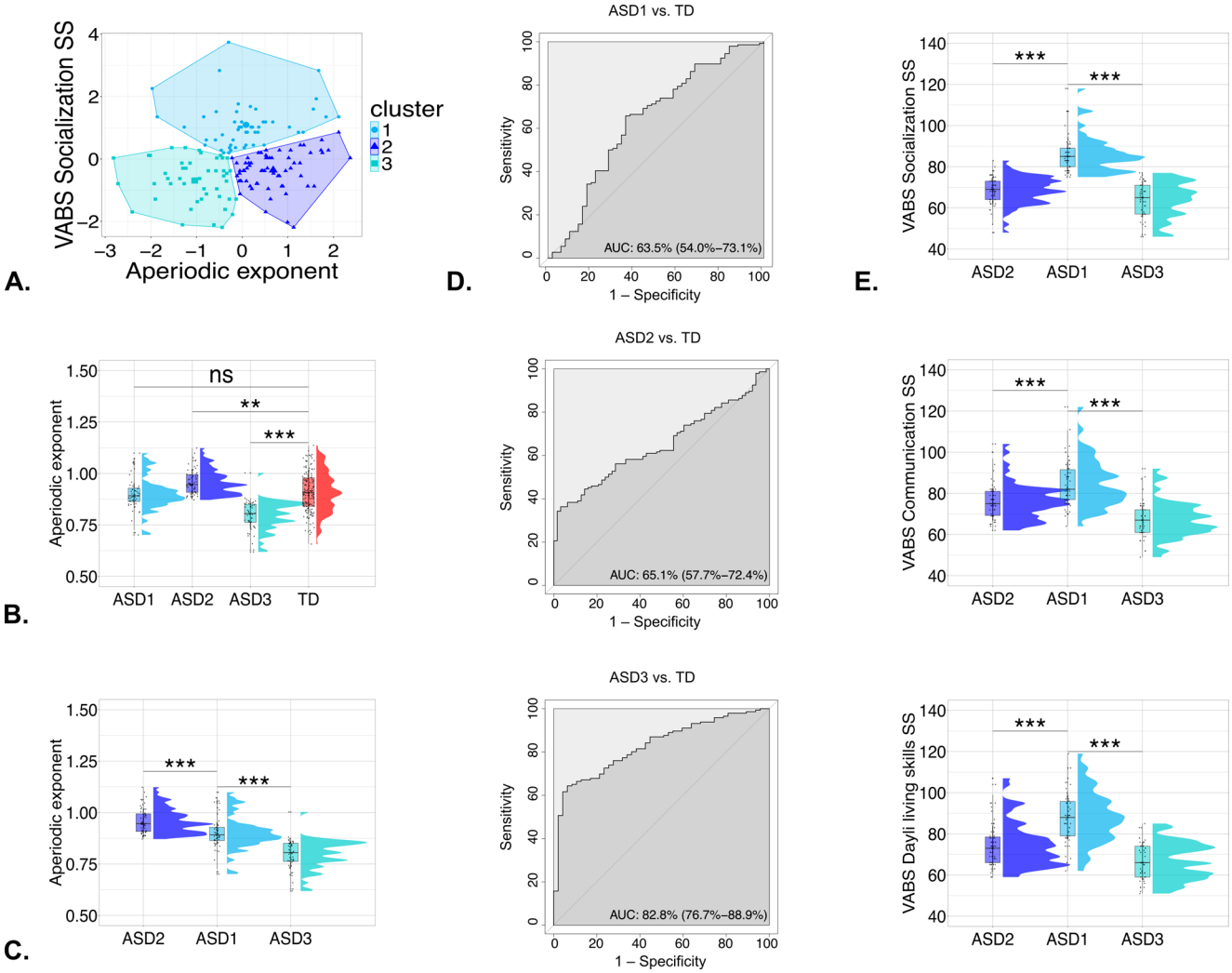

Fig. 2 Subgrouping the ASD group and age effect: (**A**) Age-related changes in aperiodic exponent in ASD and TD groups; (**B**) A visualization of the results of cluster-based analysis (cluster 1 corresponds to ASD_1, cluster 2 corresponds to ASD_2, cluster 3 corresponds to ASD_3); (**C**) Group comparisons in aperiodic exponent between ASD subgroups and TD group; (**D**) Receiver operating characteristics curves for the classification models (ASD subgroups vs. TD) for aperiodic exponent, AUC = area under the curve; (**E**) Comparisons of Vineland Adaptive Behavior Scales – 2 (VABS-2) subscores between ASD subgroups. Significance is labeled with $*p<0.05$, $**p<0.01$, $***p<0.001$, ns = non-significant. All *p*-values are FDR-corrected

had a significantly reduced aperiodic exponent, pointing to E>I neural profile (i.e., more excitation), $\beta = -15.43$, SE = 2.82, $z = -5.47$, $p<0.001$.

We applied ROC-curve analysis and calculated AUC, sensitivity, and specificity for three classification models. In general, classification power was higher for ASD subgroup discrimination compared to the whole heterogeneous ASD group. However, sensitivity remained low (Fig. 2D). AUC-values for Models 4 and 5 were ***poor*** (60% ≤ AUC < 70%), whereas for Model 6 classification was ***good*** (80% ≤ AUC < 90%), see Table 2, Models 4–6. Specificity for Models 5 and 6 (ASD subgroups with elevated I and elevated E) was high (>90%), meaning they correctly identified 94–97% of TD individuals. However, these models' sensitivity (true positive rate) was low, at 36% and 64%, respectively.

Importantly, based on cluster analysis both ASD_3 (E>I) and ASD_2 (E<I) had lower adaptive functioning in comparison to ASD_1, supporting "bell"-shape relations between E/I balance alterations and clinical phenotypes (Fig. 2E): *Socialization SS*, ASD_2 $\beta = -17.26$, SE = 1.51, $t = -11.44$, $p<0.001$; ASD_3 $\beta = -22.05$, SE = 1.62, $t = -13.62$, $p<0.001$; *Communication SS*, ASD_2 $\beta = -8.74$, SE = 1.85, $t = -4.72$, $p<0.001$; ASD_3 $\beta = -17.36$, SE = 1.98, $t = -8.79$, $p<0.001$; *Daily living skills SS*, ASD_2 $\beta = -13.84$, SE = 2.05, $t = -6.76$, $p<0.001$; ASD_3 $\beta = -21.63$, SE = 2.20, $t = -9.84$, $p<0.001$.

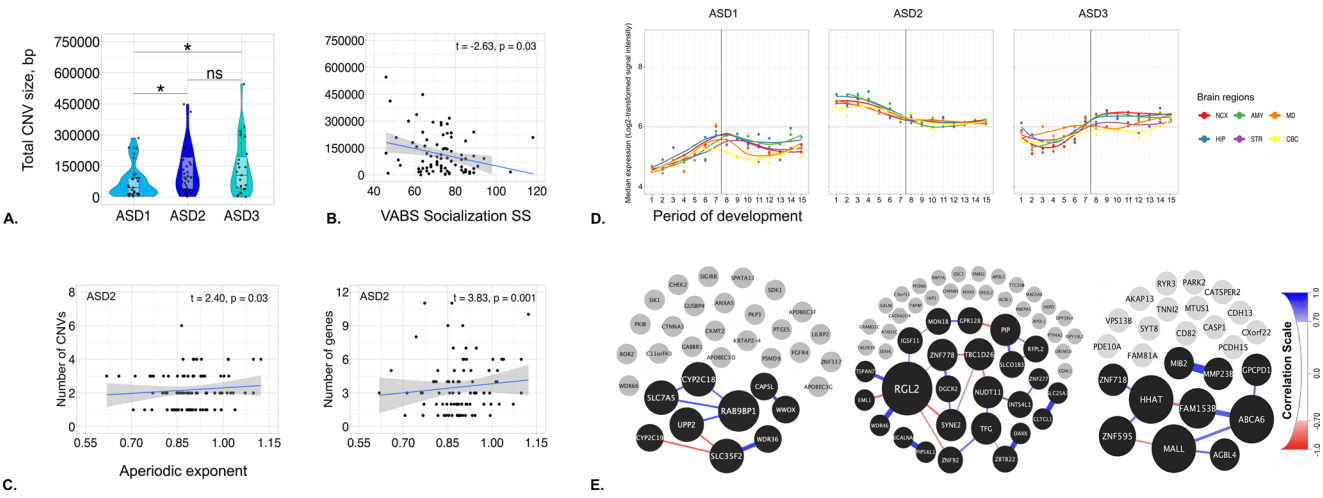

Fig. 3 Genetic profiles of ASD group: (**A**) Comparison of the total size of CNV in base pairs (bp) between ASD subgroups; (**B**) Association between the total size of CNV and VABS Socialization SS in the whole ASD group (right); (**C**) The relation of genetic variables (number of CNVs and the number of genes within CNVs) to EEG aperiodic exponent; (**D**) Median expression level of the candidate genes in the ASD subgroups by brain region and the period of development using the human BrainSpan exon-array transcriptome dataset (Kang et al. 2011). *The black vertical line* indicates birth. Log_2-transformed signal intensity ≥ 6 (the dashed red line) in at least one sample is considered positive gene expression (Kang et al. 2011). Brain regions: NCX = neocortex, AMY = amygdala, MD = mediodorsal nucleus of the thalamus, HIP = hippocampus, STR = striatum, CBC = cerebellar cortex; (**E**) Gene co-expression network analysis. Nine out of 33 genes (unique for ASD_1), 25 out of 53 genes (unique for ASD_2), and 10 out of 25 genes (unique for ASD_3) are co-expressed with at least one other candidate gene across all brain regions and the period of development with a Person correlation coefficient $r \geq 0.7$. Positive correlations are shown in *blue*, and negative ones in *red*. The greater the magnitude of the coefficient, the wider and darker are the edges. The size of a node is proportional to the number of edges that node has

Rare genic CNVs and their contribution to different neural subtypes in ASD

We analyzed CNVs to determine whether the ASD subgroups with different E/I neural profiles also have distinct genetic profiles, as well as to assess how genetics contributes to social difficulties in the whole ASD group and subgroups. Our primary measure of mutation burden was the total size of CNV per individual in base pairs (bp), as this measure had the widest distribution of data (Jack et al. 2021). To compare this measure across the ASD subgroups, we fitted a linear model with total CNV size as a dependent variable and included subgroup as a main effect (intercept corresponded to ASD_1 as a subgroup with "typical" E/I balance profile and less severe clinical phenotype). Sex was included in the model since a sex effect in total CNV size was previously identified in autistic youths (Jack et al. 2021). The results revealed a statistically significant difference between subgroups in the total CNV size (small effect size, $\eta^2 = 0.06$, 95% C.I. [0.00, 0.16]), showing that both E > I (ASD_3) and E < I (ASD_2) subgroups had larger total CNV size in comparison to ASD_1: ASD_2, $\beta = 55{,}562$, SE = 28,088, $t = 1.98$, $p = 0.05$; ASD_3, $\beta = 65{,}061$, SE = 31,070, $t = 2.09$, $p = 0.03$ (Fig. 3A). Descriptive statistics of mean values of total CNV size showed that ASD_3 with the E > I neural profile and most severe clinical phenotype had the largest total CNV size ($M = 141{,}977$ bp); ASD_2 with the E < I neural pattern and intermediate clinical profile had smaller total CNV size ($M = 130{,}877$ bp) compared to ASD_3 but larger than ASD_1 ($M = 76{,}017$ bp). However, there was no significant difference between ASD_2 and ASD_3: $H(1) = 0.004$, $p = 0.95$.

Next, we addressed linear relationships in the whole ASD group to examine the associations between genetic variables (total CNV size, number of CNVs, number of genes within CNVs per individual) and EEG aperiodic exponent as well as VABS Socialization SS. The results showed a significant relationship between total CNV size and VABS Socialization SS, so that larger total CNV size was associated with lower skills, $\beta = -2{,}489.9$, SE = 948.3, $t = -2.63$, $p = 0.03$, but not with aperiodic exponent, $\beta = 99{,}120.4$, SE = 126,769.9, $t = 0.78$, $p = 0.44$ (Fig. 3B). Other relationships were not significant: *number of CNVs*, aperiodic exponent, $\beta = 0.99$, SE = 1.23, $t = 0.80$, $p = 0.42$; VABS Socialization SS, $\beta = 0.00$, SE = 0.00, $t = 1.01$, $p = 0.47$; *number of genes*, aperiodic exponent, $\beta = 2.70$, SE = 2.80, $t = 0.97$, $p = 0.34$; VABS Socialization SS, $\beta = -0.00$, SE = 0.02, $t = -0.02$, $p = 0.98$.

Finally, as different E/I neural subtypes in ASD have different clinical profiles, we conducted the same linear analysis in each subgroup separately, as they also may have distinct genetic profiles. For each subgroup, we fitted linear models with three genetic measures as dependent variables and EEG aperiodic exponent and VABS Socialization SS as main effects. For ASD_1 and ASD_3 we did not find

any significant relationships. In contrast, for ASD_2 (E<I subtype) there were associations between EEG aperiodic exponent and *number of CNVs*, β=7.19, SE=2.99, t=2.40, p=0.03, as well as *number of genes*, β=20.98, SE=5.47, t=3.83, p=0.001 (Fig. 3C). This indicated that the higher inhibition in the ASD_2 (subgroup with increased neural inhibition profile) was related to a higher number of CNVs and a higher number of genes within CNVs.

Gene expression in the brain and its contribution to different neural subtypes in ASD

We investigated co-expression of ASD subgroups' candidate genes, as an indication of their potential functional relationships in common neural pathways relevant to ASD pathophysiology. A correlation matrix for the brain regions found in the human BrainSpan exon-array transcriptome dataset for samples representing time periods of interest to ASD development (Kang et al. 2011) (10 PCW to 2 years) was created for all genes found in the human BrainSpan dataset. The correlations for the candidate genes were extracted from the matrix and used to identify those with an absolute Pearson correlation coefficient $r \geq 0.7$ between them to determine which genes are correlated with each other. We show which genes from each ASD subgroup are found to have these correlations (Fig. 3E). Genes in light gray had no correlations with other genes with $r \geq 0.7$. Genes in black have correlations $r \geq 0.7$. Node size is proportional to the number of connections the gene has, and the width and color of the edges represent the directionality and magnitude of the Pearson correlation coefficient between the genes.

To determine whether these relationships were significant, permutation testing was conducted with 10,000 iterations of randomly selected genes from the BrainSpan dataset equal to the number of genes in each ASD subgroup (ASD_1=33, ASD_2=53, ASD_3=25). Observing the same number of correlated genes (ASD_1=9, ASD_2=25, ASD_3=10) with at least the same number of correlations/gene (N_{ASD1} = 0.89, N_{ASD2} = 1.04, N_{ASD3} = 0.9) is trending towards significance for subgroups ASD_2 and ASD_3 but not ASD_1 (ASD_1 p=0.3818, ASD_2 p=0.0968, ASD_3 p=0.0911). Observing the same number of genes with a mean correlation coefficient of at least that for each subgroup (r_{ASD1} = 0.744, r_{ASD2} = 0.786, r_{ASD3} = 0.771) was significant for subgroups ASD_2 and ASD_3 but not ASD_1 (ASD_1 p=0.4305, ASD_2 p=0.0002, ASD_3 p=0.0225). Meeting both thresholds resulted in significance for ASD_2 and ASD_3 but not ASD_1 (ASD_1 p=0.3165, ASD_2 p=0.0002, ASD_3 p=0.0019).

Using the human BrainSpan exon-array transcriptome dataset, we plotted the median expression level of the correlated genes as a group for each ASD subgroup for all the brain regions available from embryonic to late adulthood stages. As shown by the expression profile in Fig. 3D, the candidate genes in the three ASD subgroups had very different expression trajectories in the brain over the lifespan. The ASD_1-correlated genes showed overall lack of brain gene expression (log_2-transformed signal intensity<6). By contrast, ASD_2-correlated genes demonstrated overall positive brain gene expression through life with higher levels *prenatally*. The ASD_3-correlated genes revealed positive brain gene expression largely *postnatally*. Both ASD_2- and ASD_3- (with E<I and E>I neural profiles) correlated genes are expressed in the brain during time periods proposed to be critical for ASD onset. However, the patterns of gene expression are distinct with evidence of more *prenatal* (ASD_2) vs. *postnatal* (ASD_3) expression. As it is shown by the expression profiles, in ASD_2, the candidate genes are expressed in all brain regions, whereas in ASD_3 (the subgroup with the most altered cognitive phenotype), the candidate genes are more highly expressed in neocortex, amygdala, and hippocampus which, according to numerous studies, are the core regions of the "social brain" (Arutiunian et al. 2023; Banker et al. 2021; Dunbar 2024).

Discussion

The present study addressed E/I imbalance in ASD and its relation to a core autism symptom domain, i.e., adaptive social function. Using a parameterization approach to calculate periodic and aperiodic components of the EEG spectral power during resting-state in a large sex-balanced sample of participants with and without ASD, we showed that the aperiodic exponent (a primary measure of E/I balance) was reduced in youth with ASD, suggesting elevated excitation. Furthermore, this reduction was associated with lower adaptive social skills. However, subgrouping of the ASD sample demonstrated both E>I and E<I neural profiles (as well as a neural profile similar to that of TD participants), and both profiles characterized by E/I imbalance were related to worse clinical phenotype. Moreover, genetics analysis showed that the ASD subgroups had different profiles with respect to total CNV size per individual and the expression of candidate genes in the brain. This approach to subgroup identification can result in higher accuracy in group discriminative power as well as revealing clinically meaningful neural subtypes within the heterogeneous ASD population. It may also explain inconsistent results in the existing literature as variability in sample composition by neural subgroup will influence the main group discrimination effect.

Similar to previous findings, we showed that the raw gamma power was elevated in the ASD group compared to TD controls when accounting for age and sex (Neo et

al. 2023). Gamma oscillations are one index of E/I balance, arising from the inhibition of pyramidal cells via binding to the inhibitory GABAergic neurotransmitter (Cardin et al. 2009; Espinoza et al. 2018; Sohal et al. 2009). Therefore, increased spectral power at the gamma frequency range may reflect increased E/I ratio (Sohal and Rubenstein 2019). However, by applying the parameterization algorithm and separating raw EEG spectral power into periodic and aperiodic components, we showed that while aperiodic-adjusted gamma power did not differ between groups of youth with and without ASD, the aperiodic exponent was reduced in the ASD group. Several recent studies have revealed that the aperiodic exponent rather than raw gamma power reflects the E/I balance, and that the slope characteristics can indicate whether the neural circuit has increased E (lower exponent) or increased I (higher exponent) (Donoghue et al. 2020; Ostlund et al. 2022). Thus, reduced aperiodic exponent in the ASD group suggests increased E over I which, in turn, may result in increased 'noise' in the cortex, impacting synaptic plasticity during development and resulting in less effective neural processing (Contractor et al. 2021; Sohal and Rubenstein 2019; Tang et al. 2021). Elevated excitatory activity in the autistic brain may also explain a high rate of epilepsy in this population (Besag 2018). Importantly, social dysfunction in the ASD group was related to the aperiodic exponent (but not to the raw gamma power or aperiodic-adjusted gamma power), such that a lower exponent (higher E) was associated with lower social skills.

Although the aperiodic exponent was altered in autistic youth, we observed similar age-related decreases in this measure across both the ASD and TD groups of participants. This decrease started after 12.5 years of age in both groups and, presumably, was related to less cortical inhibition with age (Ostlund et al. 2022). Our findings are consistent with existing studies that show a similar pattern, suggesting age-related changes in E/I balance towards less inhibition with age and accounting for a normative redistribution of spectral power from lower to higher levels over development (Ostlund et al. 2022).

Previous comprehensive studies of E/I imbalance in ASD have proposed that E>I is not the only possible neural profile but that there can be an opposite pattern as well, E<I (Antoine et al. 2019; Dickinson et al. 2016). To the best of our knowledge, there is only one EEG study that addressed the clustering of the ASD group based on the E/I balance profiles (Bertelsen et al. 2024). In that study, two ASD subtypes were identified, i.e., with elevated E and elevated I when compared to the control group. Given the heterogeneous nature of the ASD population and the relationship between aperiodic exponent (a measure of E/I balance) and the social skills of autistic youth, we conducted cluster-based analysis in the ASD group with respect to exponent and social skills. Our study revealed three ASD subtypes concerning E/I balance: "typical", E>I, and E<I neural profiles compared to the TD group. Importantly, the two ASD subgroups with E/I imbalance had lower social, communication, and daily living skills in comparison to the ASD subgroup with "typical" E/I balance, suggesting "bell"-shaped brain-behavior relationships.

Our unbiased genome-wide CNV analysis aimed to reveal whether the ASD subgroups with different E/I balance subtypes also have distinct genetic profiles. First, we identified that the two ASD subgroups with altered E/I balance had larger total CNV size per individual compared to the ASD subgroup with "typical" E/I balance profile. Also, in the whole ASD group, the larger total CNV size was associated with lower social skills. CNVs are genomic duplications or deletions that are a significant source of genetic disorders (Auwerx et al. 2024). Our findings are consistent with previous studies, demonstrating that larger CNVs are related to behavioral and brain abnormalities in different psychiatric and neurological disorders (Arutiunian et al. 2026; Cooper et al. 2011; Gupta et al. 2017; Mefford et al., 2010; Sebat et al. 2007; Walsh et al. 2008). In addition, we identified that only in the ASD subgroup with E<I neural profile there were linear relationships of the number of CNVs and number of genes within CNVs to the E/I balance neural measure. In other words, larger genomic alterations were related to overall lower circuit activity in the ASD subgroup with increased inhibition. This suggests that, although the two E/I imbalance ASD subgroups did not significantly differ in total CNV size, the functional specificity of alterations in the genome and their impact on neural circuits is distinct.

The findings from gene expression analysis made an additional significant contribution to the characterization of ASD subgroups. For each ASD subgroup, we identified unique genes within the CNVs and assessed the expression level of correlated genes for all brain regions over the lifespan. In general, gene expression patterns were different among the ASD subgroups. The ASD subgroup with "typical" E/I balance showed an overall lack of expression of the candidate genes compared to the other two subgroups with E/I balance alterations. In the E<I subgroup, the candidate genes were expressed in all brain regions, whereas in the E>I subgroup with the most altered clinical phenotype, the candidate genes were more highly expressed in neocortex, amygdala, and hippocampus which, according to the number of neuroimaging studies, are the main regions that are involved in core functions in the "social brain" and, thus, in core symptoms of ASD (Arutiunian et al. 2023; Banker et al. 2021; Dunbar 2024).

Importantly, the trajectories of gene expression were distinct in the ASD subgroups during time periods that were thought to be critical for the development of ASD. The

ASD E>I neural subtype had higher *postnatal* gene expression, whereas the ASD E<I neural subtype demonstrated higher *prenatal* gene expression. These pre- vs. postnatal gene expression profiles in the brain, leading to opposite E/I neural imbalance subtypes in ASD, can shed light on the distinct developmental atypicalities in the neurocircuits associated with the core autistic feature, i.e., social skills. Recent genome-wide association studies that examined idiopathic ASD have revealed distinct clusters of brain-related genes within rare CNVs that are expressed in different developmental periods with evidence of pre- vs. postnatal gene clusters (Courchesne et al. 2020). These clusters associated with different developmental periods have different functional specificity in brain development. For instance, genes that are expressed largely prenatally are involved in proliferation, migration, cell fate specification, neurite overgrowth, and formation of the cortical layers, whereas the genes that are mainly expressed postnatally are related to synaptogenesis, axonal growth, and wiring of the cortex (Chen et al. 2015; Courchesne et al. 2019; Grove et al. 2019). Several genetic studies addressing the identified of pre- vs. postnatal gene clusters have raised the question of whether the disruption of these different clusters results in distinct subtypes of ASD (Courchesne et al. 2019, 2020). In this study, we demonstrated that pre- vs. postnatal brain gene expression profiles are associated with opposite neural subtypes, revealing that the ASD subgroup with overall lower circuit activity (E<I) had a largely prenatal gene expression profile, whereas the ASD subgroup with overall higher circuit activity (E>I) had a largely postnatal gene expression profile.

Limitations

We note several study design choices that likely impact our results. First, although this dataset is one of the largest datasets with genetics, EEG neural functioning, and mental health in autistic youth, it includes primarily average-to-high cognitive ability individuals. Inclusion of individuals with high support needs or lower cognitive ability may shift results, although we propose that including the full spectrum of autistic individuals would likely enhance the subgroup membership findings. Second, the study focused on 8–17-year-old youth with ASD and given age-based changes in our E/I metrics, neural subtyping including different developmental periods is needed. Future studies would benefit from including additional methodological approaches, such as magnetic resonance spectroscopy, to measure the level of glutamate and GABA in autistic subgroups as this would link these results to neurotransmitter levels.

Conclusions

Development of neural biomarkers for diagnostic and clinical trial purposes is one of the central challenges in ASD research (Webb et al. 2023). A significant challenge is that ASD is a highly heterogeneous population; to develop biomarkers there is a need to identify clinically meaningful neural subtypes within this population. In our study, we revealed different E/I balance neural subtypes in the ASD group with the opposite E/I ratios, i.e., "typical", E>I, and E<I profiles. Importantly, altered E/I balance subtypes compared to the "typical" E/I balance subgroup had more altered clinical phenotypes and distinct genetic profiles with the evidence of more pre- vs. postnatal gene expression in the brain. This suggests that the proposed clustering approach is relevant for identifying clinically meaningful neural subtypes within the ASD group with distinct genetic profiles. In addition, this approach allows us to stratify one ASD subgroup from the TD group with good discriminatory performance (ASD_3, AUC = 82.8%). However, although the ASD_3 subgroup was discriminated from the TD group with high specificity and good overall classification performance, the more modest sensitivity indicates that resting-state EEG alone does not identify all individuals assigned to this subgroup. This is not unexpected, as subgroup membership was established using a multimodal clustering approach that incorporated both EEG and behavioral measures, whereas the classification analysis evaluated the discriminative performance of resting-state EEG alone. Accordingly, our findings do not support the use of resting-state EEG as a stand-alone screening or diagnostic tool. Instead, they suggest that resting-state EEG provides a biologically informative marker that can contribute to multimodal stratification approaches aimed at identifying more homogeneous neurobiological subgroups within the heterogeneous ASD population.

Supplementary Information The online version contains supplementary material available at https://doi.org/10.1007/s00702-026-03283-0.

Acknowledgements We wish to thank the families, parents, and children who participated in our study at our four data collection sites. The ACE GENDAAR Network additionally included contributions from: Katy Ankenman MSW, Elizabeth Aylward PhD, Veronica Kang PhD, Erin J. Libsack PhD, and Désirée Lussier-Lévesque PhD who were formerly at Seattle Children's Research Institute; Sarah Corrigan MA and Waylon Howard PhD who are currently at Seattle Children's Research Institute; Laura A. Edwards PhD and Jack Keller who were formerly at Boston Children's Hospital; Rachael Tillman PhD who was formerly at Yale Child Study Center; Scott Huberty PhD who was formerly at UCLA; Zachary Jacokes who is currently at University of Virginia; Carinna Torgerson who is currently at USC; and Charles Nelson who is currently at Boston Children's Hospital and Harvard Medical School.

Author contributions RB, SB, MD, SJ, JMCP, AN, JVH, KP, SJW,

and ARG designed the project; MS, EN, HB contributed to acquisition; VA, CS, HB, SJW and ARG contributed to EEG and genetic analysis; VA, CS, MS, EN, AJ, SJW and ARG contributed to interpretation of data for the work; all authors provided input in to the drafting the work and all authors provided final approval of the version to be published and agree to be accountable for all aspects of the work.

Funding Funding was provided by the R01MH10028 (NIMH ACE Network, Pelphrey), R01MH117982 (Dapretto/Pelphrey), and the University of Washington Intellectual and Developmental Disabilities Research Center (U54HD083091).

Data availability The behavioral and EEG data from the current study are available via the National Institute of Mental Health Data Archive Data Collection #2021. All genetic and biospecimen data from ACE study participants were contributed to the NIMH Repository and Genomics Resource (https://www.nimhgenetics.org) as well as archived through Sampled, Inc. (http://sampled.com), Infinity BiologiX/RUCDR.

Declarations

Competing interests James C. McPartland consults or has consulted with Customer Value Partners, Bridgebio, Determined Health, Apple, and BlackThorn Therapeutics, has received research funding from Janssen Research and Development, serves on the Scientific Advisory Boards of Pastorus and Modern Clinics, and receives royalties from Guilford Press, Lambert, Oxford, and Springer.The remaining authors have no conflict of interest to declare.

Ethics approval and consent to participate The study was approved by the Yale Institutional Review Board, the UCLA Office of Human Research Protection Program, Boston Children's Hospital Institutional Review Board, USC Office for the Protection of Research Subjects, and the University of Virginia Institutional Review Board for Health Sciences Research. All procedures performed were in accordance with the Declaration of Helsinki. All minor children provided verbal assent to participate in the study and were informed that they can withdraw from the study at any time during the experiment. A written consent form was obtained from a parent of each child participating in the study.

Consent for publication Not applicable.

References

Affymetrix (2005) Exon Array Background Correction

Agetsuma M, Hamm JP, Tao K, Fujisawa S, Yuste R (2018) Parvalbumin-Positive Interneurons Regulate Neuronal Ensembles in Visual Cortex. Cereb Cortex 28:1831–1845. https://doi.org/10.1093/cercor/bhx169

American Psychiatric Association (2000) Diagnostic and statistical manual of mental disorders: DSM-IV-TR, 4th ed. Author, Washington, DC

American Psychiatric Association (2013) Diagnostic and statistical manual of mental disorders: DSM-5, 5th ed. American Psychiatric Publication, Washington, DC; London

Antoine MW, Langberg T, Schnepel P, Feldman DE (2019) Increased Excitation-Inhibition Ratio Stabilizes Synapse and Circuit Excitability in Four Autism Mouse Models. Neuron 101:648–661e4. https://doi.org/10.1016/j.neuron.2018.12.026

Arutiunian V, Davydova E, Pereverzeva D, Sorokin A, Tyushkevich S, Mamokhina U, Danilina K, Dragoy O (2023) Reduced grey matter volume of amygdala and hippocampus is associated with the severity of autistic symptoms and language abilities in school-aged children with Autism Spectrum Disorder: an exploratory study. Brain Struct Funct 228:1573–1579. https://doi.org/10.1007/s00429-023-02660-9

Arutiunian V, Santhosh M, Neuhaus E, Borland H, Tompkins C, Bernier RA, Bookheimer SY, Dapretto M, Gupta AR, Jack A, Jeste S, McPartland JC, Naples A, Van Horn JD, Pelphrey KA, Webb SJ (2024) The relationship between gamma-band neural oscillations and language skills in youth with autism spectrum disorder and their first-degree relatives. Mol Autism 15:19. https://doi.org/10.1186/s13229-024-00598-1

Arutiunian V, Opdahl M, Sullivan CAW, Santhosh M, Neuhaus E, Borland H, Bernier RA, Bookheimer SY, Dapretto M, Jack A, Jeste S, McPartland JC, Naples A, Van Horn JD, Pelphrey KA, Webb SJ, Gupta AR (2026) Number of alpha peaks in the electroencephalogram is associated with clinical phenotype and copy number variants in youths with autism. Biol Psychiatry Cogn Neurosci Neuroimaging 11:300–309. https://doi.org/10.1016/j.bpsc.2025.10.001

Auwerx C, Jõeloo M, Sadler MC, Tesio N, Ojavee S, Clark CJ, Mägi R, Estonian Biobank Research Team, Reymond A, Kutalik Z (2024) Rare copy-number variants as modulators of common disease susceptibility. Genome Med 16:5. https://doi.org/10.1186/s13073-023-01265-5

Banker SM, Gu X, Schiller D, Foss-Feig JH (2021) Hippocampal contributions to social and cognitive deficits in autism spectrum disorder. Trends Neurosci 44:793–807. https://doi.org/10.1016/j.tins.2021.08.005

Bartos M, Vida I, Jonas P (2007) Synaptic mechanisms of synchronized gamma oscillations in inhibitory interneuron networks. Nat Rev Neurosci 8:45–56. https://doi.org/10.1038/nrn2044

Bates D, Mächler M, Bolker B, Walker S (2015) Fitting linear mixed-effects models using lme4. J Stat Softw 67:1–48. https://doi.org/10.18637/jss.v067.i01

Ben-Shachar MS, Lüdecke D, Makowski D (2020) Effectsize: estimation of effect size indices and standardized parameters. J Open Source Softw 5:2815. https://doi.org/10.21105/joss.02815

Bertelsen N, Mancini G, Sastre-Yagüe D, Vitale A, Lorenz GM, Malerba SB, Bolis D, Mandelli V, Martínez-Cañada P, Gozzi A, Panzeri S, Lombardo MV (2024) Electrophysiologically-defined excitation-inhibition autism neurosubtypes. https://doi.org/10.1101/2023.11.22.23298729

Besag FM (2018) Epilepsy in patients with autism: links, risks and treatment challenges. Neuropsychiatr Dis Treat 14:1–10. https://doi.org/10.2147/NDT.S120509

Bhaskaran AA, Gauvrit T, Vyas Y, Bony G, Ginger M, Frick A (2023) Endogenous noise of neocortical neurons correlates with atypical sensory response variability in the *Fmr1−/y* mouse model of autism. Nat Commun 14:7905. https://doi.org/10.1038/s41467-023-43777-z

Buzsáki G, Wang X-J (2012) Mechanisms of gamma oscillations. Annu Rev Neurosci 35:203–225. https://doi.org/10.1146/annurev-neuro-062111-150444

Cardin JA, Carlén M, Meletis K, Knoblich U, Zhang F, Deisseroth K, Tsai L-H, Moore CI (2009) Driving fast-spiking cells induces gamma rhythm and controls sensory responses. Nature 459:663–667. https://doi.org/10.1038/nature08002

Carlén M, Meletis K, Siegle JH, Cardin JA, Futai K, Vierling-Claassen D, Rühlmann C, Jones SR, Deisseroth K, Sheng M, Moore CI, Tsai L-H (2012) A critical role for NMDA receptors in parvalbumin interneurons for gamma rhythm induction and behavior. Mol Psychiatry 17:537–548. https://doi.org/10.1038/mp.2011.31

Chao H-T, Chen H, Samaco RC, Xue M, Chahrour M, Yoo J, Neul JL, Gong S, Lu H-C, Heintz N, Ekker M, Rubenstein JLR, Noebels JL, Rosenmund C, Zoghbi HY (2010) Dysfunction in GABA signalling mediates autism-like stereotypies and Rett syndrome phenotypes. Nature 468:263–269. https://doi.org/10.1038/nature09582

Chen Y, Huang W-C, Séjourné J, Clipperton-Allen AE, Page DT (2015) Pten Mutations Alter Brain Growth Trajectory and Allocation of Cell Types through Elevated β-Catenin Signaling. J Neurosci 35:10252–10267. https://doi.org/10.1523/JNEUROSCI.5272-14.2015

Cline MS, Smoot M, Cerami E, Kuchinsky A, Landys N, Workman C, Christmas R, Avila-Campilo I, Creech M, Gross B, Hanspers K, Isserlin R, Kelley R, Killcoyne S, Lotia S, Maere S, Morris J, Ono K, Pavlovic V, Pico AR, Vailaya A, Wang P-L, Adler A, Conklin BR, Hood L, Kuiper M, Sander C, Schmulevich I, Schwikowski B, Warner GJ, Ideker T, Bader GD (2007) Integration of biological networks and gene expression data using Cytoscape. Nat Protoc 2:2366–2382. https://doi.org/10.1038/nprot.2007.324

Constantino JN (2012) Social Responsiveness Scale, second edition (SRS-2). Western Psychological Services

Contractor A, Ethell IM, Portera-Cailliau C (2021) Cortical interneurons in autism. Nat Neurosci 24:1648–1659. https://doi.org/10.1038/s41593-021-00967-6

Cooper GM, Coe BP, Girirajan S, Rosenfeld JA, Vu TH, Baker C, Williams C, Stalker H, Hamid R, Hannig V, Abdel-Hamid H, Bader P, McCracken E, Niyazov D, Leppig K, Thiese H, Hummel M, Alexander N, Gorski J, Kussmann J, Shashi V, Johnson K, Rehder C, Ballif BC, Shaffer LG, Eichler EE (2011) A copy number variation morbidity map of developmental delay. Nat Genet 43:838–846. https://doi.org/10.1038/ng.909

Core Team R (2023) R: A Language and Environment for Statistical Computing

Courchesne E, Pramparo T, Gazestani VH, Lombardo MV, Pierce K, Lewis NE (2019) The ASD living biology: from cell proliferation to clinical phenotype. Mol Psychiatry 24:88–107. https://doi.org/10.1038/s41380-018-0056-y

Courchesne E, Gazestani VH, Lewis NE (2020) Prenatal origins of ASD: the when, what, and how of ASD development. Trends Neurosci 43:326–342. https://doi.org/10.1016/j.tins.2020.03.005

Delattre V, La Mendola D, Meystre J, Markram H, Markram K (2013) Nlgn4 knockout induces network hypo-excitability in juvenile mouse somatosensory cortex in vitro. Sci Rep 3:2897. https://doi.org/10.1038/srep02897

Dickinson A, Jones M, Milne E (2016) Measuring neural excitation and inhibition in autism: different approaches, different findings and different interpretations. Brain Res 1648:277–289. https://doi.org/10.1016/j.brainres.2016.07.011

Donoghue T, Haller M, Peterson EJ, Varma P, Sebastian P, Gao R, Noto T, Lara AH, Wallis JD, Knight RT, Shestyuk A, Voytek B (2020) Parameterizing neural power spectra into periodic and aperiodic components. Nat Neurosci 23:1655–1665. https://doi.org/10.1038/s41593-020-00744-x

Dunbar RIM (2024) The social brain hypothesis - thirty years on. Ann Hum Biol 51:2359920. https://doi.org/10.1080/03014460.2024.2359920

Elliott CD (2007) Differential Ability Scales, second edition. The Psychological Corporation, San Antonio, TX

Espinoza C, Guzman SJ, Zhang X, Jonas P (2018) Parvalbumin+ interneurons obey unique connectivity rules and establish a powerful lateral-inhibition microcircuit in dentate gyrus. Nat Commun 9:4605. https://doi.org/10.1038/s41467-018-06899-3

Gabard-Durnam LJ, Mendez Leal AS, Wilkinson CL, Levin AR (2018) The Harvard automated processing pipeline for electroencephalography (HAPPE): standardized processing software for developmental and high-artifact data. Front Neurosci. https://doi.org/10.3389/fnins.2018.00097

Gabard-Durnam LJ, Wilkinson C, Kapur K, Tager-Flusberg H, Levin AR, Nelson CA (2019) Longitudinal EEG power in the first postnatal year differentiates autism outcomes. Nat Commun 10:4188. https://doi.org/10.1038/s41467-019-12202-9

Gandal MJ, Edgar JC, Ehrlichman RS, Mehta M, Roberts TPL, Siegel SJ (2010) Validating γ oscillations and delayed auditory responses as translational biomarkers of autism. Biol Psychiatry 68:1100–1106. https://doi.org/10.1016/j.biopsych.2010.09.031

Gao R, Peterson EJ, Voytek B (2017) Inferring synaptic excitation/inhibition balance from field potentials. NeuroImage 158:70–78. https://doi.org/10.1016/j.neuroimage.2017.06.078

Gatto CL, Broadie K (2010) Genetic controls balancing excitatory and inhibitory synaptogenesis in neurodevelopmental disorder models. Front Synaptic Neurosci 2:4. https://doi.org/10.3389/fnsyn.2010.00004

Gilman SR, Iossifov I, Levy D, Ronemus M, Wigler M, Vitkup D (2011) Rare de novo variants associated with autism implicate a large functional network of genes involved in formation and function of synapses. Neuron 70:898–907. https://doi.org/10.1016/j.neuron.2011.05.021

Grove J, Ripke S, Als TD, Mattheisen M, Walters RK, Won H, Pallesen J, Agerbo E, Andreassen OA, Anney R, Awashti S, Belliveau R, Bettella F, Buxbaum JD, Bybjerg-Grauholm J, Bækvad-Hansen M, Cerrato F, Chambert K, Christensen JH, Churchhouse C, Dellenvall K, Demontis D, De Rubeis S, Devlin B, Djurovic S, Dumont AL, Goldstein JI, Hansen CS, Hauberg ME, Hollegaard MV, Hope S, Howrigan DP, Huang H, Hultman CM, Klei L, Maller J, Martin J, Martin AR, Moran JL, Nyegaard M, Nærland T, Palmer DS, Palotie A, Pedersen CB, Pedersen MG, d Poterba T, Poulsen JB, Pourcain BS, Qvist P, Rehnström K, Reichenberg A, Reichert J, Robinson EB, Roeder K, Roussos P, Saemundsen E, Sandin S, Satterstrom FK, Davey Smith G, Stefansson H, Steinberg S, Stevens CR, Sullivan PF, Turley P, Walters GB, Xu X, Autism Spectrum Disorder Working Group of the Psychiatric Genomics Consortium, BUPGEN, Major Depressive Disorder Working Group of the Psychiatric Genomics Consortium, 23andMe Research Team, Stefansson K, Geschwind DH, Nordentoft M, Hougaard DM, Werge T, Mors O, Mortensen PB, Neale BM, Daly MJ, Børglum AD (2019) Identification of common genetic risk variants for autism spectrum disorder. Nat Genet 51:431–444. https://doi.org/10.1038/s41588-019-0344-8

Gupta AR, Westphal A, Yang DYJ, Sullivan CAW, Eilbott J, Zaidi S, Voos A, Vander Wyk BC, Ventola P, Waqar Z, Fernandez TV, Ercan-Sencicek AG, Walker MF, Choi M, Schneider A, Hedderly T, Baird G, Friedman H, Cordeaux C, Ristow A, Shic F, Volkmar FR, Pelphrey KA (2017) Neurogenetic analysis of childhood disintegrative disorder. Mol Autism 8:19. https://doi.org/10.1186/s13229-017-0133-0

Hennig C (2026) fpc: Flexible Procedures for Clustering

Hollestein V, Poelmans G, Forde NJ, Beckmann CF, Ecker C, Mann C, Schäfer T, Moessnang C, Baumeister S, Banaschewski T, Bourgeron T, Loth E, Dell'Acqua F, Murphy DGM, Puts NA, Tillmann J, Charman T, Jones EJH, Mason L, Ambrosino S, Holt R, Bölte S, Buitelaar JK, Naaijen J (2023) Excitatory/inhibitory imbalance in autism: the role of glutamate and GABA gene-sets in symptoms and cortical brain structure. Transl Psychiatry 13:18. https://doi.org/10.1038/s41398-023-02317-5

Hunter JD (2007) Matplotlib: a 2D graphics environment. Comput Sci Eng 9:90–95. https://doi.org/10.1109/MCSE.2007.55

Jack A, Sullivan CAW, Aylward E, Bookheimer SY, Dapretto M, Gaab N, Van Horn JD, Eilbott J, Jacokes Z, Torgerson CM, Bernier RA, Geschwind DH, McPartland JC, Nelson CA, Webb SJ, Pelphrey KA, Gupta AR, GENDAAR Consortium (2021) A neurogenetic

analysis of female autism. Brain 144:1911–1926. https://doi.org/10.1093/brain/awab064

Kang HJ, Kawasawa YI, Cheng F, Zhu Y, Xu X, Li M, Sousa AMM, Pletikos M, Meyer KA, Sedmak G, Guennel T, Shin Y, Johnson MB, Krsnik Z, Mayer S, Fertuzinhos S, Umlauf S, Lisgo SN, Vortmeyer A, Weinberger DR, Mane S, Hyde TM, Huttner A, Reimers M, Kleinman JE, Sestan N (2011) Spatio-temporal transcriptome of the human brain. Nature 478:483–489. https://doi.org/10.1038/nature10523

Kassambara A, Mundt F (2020) Factoextra: extract and visualize the results of multivariate data analyses

Kjelgaard MM, Tager-Flusberg H (2001) An Investigation of Language Impairment in Autism: Implications for Genetic Subgroups. Lang Cogn Process 16:287–308. https://doi.org/10.1080/01690960042000058

Le Magueresse C, Monyer H (2013) GABAergic interneurons shape the functional maturation of the cortex. Neuron 77:388–405. https://doi.org/10.1016/j.neuron.2013.01.011

Levin AR, Nelson CA (2015) Inhibition-Based Biomarkers for Autism Spectrum Disorder. Neurotherapeutics 12:546–552. https://doi.org/10.1007/s13311-015-0350-1

Levin AR, Méndez Leal AS, Gabard-Durnam LJ, O'Leary HM (2018) BEAPP: the batch electroencephalography automated processing platform. Front Neurosci. https://doi.org/10.3389/fnins.2018.00513

Levin AR, Naples AJ, Scheffler AW, Webb SJ, Shic F, Sugar CA, Murias M, Bernier RA, Chawarska K, Dawson G, Faja S, Jeste S, Nelson CA, McPartland JC, Şentürk D, Autism Biomarkers Consortium for Clinical Trials (2020) Day-to-day test-retest reliability of EEG profiles in children with autism spectrum disorder and typical development. Front Integr Neurosci. https://doi.org/10.3389/fnint.2020.00021

Lord C, Rutter M, DiLavore PC, Risi S, Gotham K, Bishop S (2012) Autism Diagnostic Observation Schedule, second edition (ADOS-2) manual (part I): modules 1–4. Western Psychological Services, Torrance, CA

Matson JL, Rieske RD, Williams LW (2013) The relationship between autism spectrum disorders and attention-deficit/hyperactivity disorder: An overview. Res Dev Disabil 34:2475–2484. https://doi.org/10.1016/j.ridd.2013.05.021

Mefford HC, Muhle H, Ostertag P, von Spiczak S, Buysse K, Baker C, Franke A, Malafosse A, Genton P, Thomas P, Gurnett CA, Schreiber S, Bassuk AG, Guipponi M, Stephani U, Helbig I, Eichler EE (2010) Genome-wide copy number variation in epilepsy: novel susceptibility loci in idiopathic generalized and focal epilepsies. PLoS Genet 6:e1000962. https://doi.org/10.1371/journal.pgen.1000962

Nahm FS (2022) Receiver operating characteristic curve: overview and practical use for clinicians. Korean J Anesthesiol 75:25–36. https://doi.org/10.4097/kja.21209

Neo WS, Foti D, Keehn B, Kelleher B (2023) Resting-state EEG power differences in autism spectrum disorder: a systematic review and meta-analysis. Transl Psychiatry 13:389. https://doi.org/10.1038/s41398-023-02681-2

Ostlund B, Donoghue T, Anaya B, Gunther KE, Karalunas SL, Voytek B, Pérez-Edgar KE (2022) Spectral parameterization for studying neurodevelopment: how and why. Dev Cogn Neurosci 54:101073. https://doi.org/10.1016/j.dcn.2022.101073

Polyak A, Kubina RM, Girirajan S (2015) Comorbidity of intellectual disability confounds ascertainment of autism: implications for genetic diagnosis. Am J Med Genet B Neuropsychiatr Genet 168:600–608. https://doi.org/10.1002/ajmg.b.32338

Purcell S, Neale B, Todd-Brown K, Thomas L, Ferreira MAR, Bender D, Maller J, Sklar P, de Bakker PIW, Daly MJ, Sham PC (2007) PLINK: a tool set for whole-genome association and population-based linkage analyses. Am J Hum Genet 81:559–575. https://doi.org/10.1086/519795

Robin X, Turck N, Hainard A, Tiberti N, Lisacek F, Sanchez J-C, Müller M (2011) pROC: an open-source package for R and S+to analyze and compare ROC curves. BMC Bioinformatics 12:77. https://doi.org/10.1186/1471-2105-12-77

Rojas DC, Wilson LB (2014) γ-band abnormalities as markers of autism spectrum disorders. Biomark Med 8:353–368. https://doi.org/10.2217/bmm.14.15

Rubenstein JLR, Merzenich MM (2003) Model of autism: increased ratio of excitation/inhibition in key neural systems. Genes Brain Behav 2:255–267. https://doi.org/10.1034/j.1601-183x.2003.00037.x

Rutter M, Bailey A, Lord C (2003a) Social Communication Questionnaire. Western Psychological Services, Torrance, CA

Rutter M, Le Couteur A, Lord C (2003b) ADI-R: Autism Diagnostic Interview-Revised. Western Psychological Services, Los Angeles, CA

Sanders SJ, Ercan-Sencicek AG, Hus V, Luo R, Murtha MT, Moreno-De-Luca D, Chu SH, Moreau MP, Gupta AR, Thomson SA, Mason CE, Bilguvar K, Celestino-Soper PBS, Choi M, Crawford EL, Davis L, Wright NRD, Dhodapkar RM, DiCola M, DiLullo NM, Fernandez TV, Fielding-Singh V, Fishman DO, Frahm S, Garagaloyan R, Goh GS, Kammela S, Klei L, Lowe JK, Lund SC, McGrew AD, Meyer KA, Moffat WJ, Murdoch JD, O'Roak BJ, Ober GT, Pottenger RS, Raubeson MJ, Song Y, Wang Q, Yaspan BL, Yu TW, Yurkiewicz IR, Beaudet AL, Cantor RM, Curland M, Grice DE, Günel M, Lifton RP, Mane SM, Martin DM, Shaw CA, Sheldon M, Tischfield JA, Walsh CA, Morrow EM, Ledbetter DH, Fombonne E, Lord C, Martin CL, Brooks AI, Sutcliffe JS, Cook EH, Geschwind D, Roeder K, Devlin B, State MW (2011) Multiple recurrent de novo CNVs, including duplications of the 7q11.23 Williams syndrome region, are strongly associated with autism. Neuron 70:863–885. https://doi.org/10.1016/j.neuron.2011.05.002

Sanders SJ, He X, Willsey AJ, Ercan-Sencicek AG, Samocha KE, Cicek AE, Murtha MT, Bal VH, Bishop SL, Dong S, Goldberg AP, Jinlu C, Keaney JF, Klei L, Mandell JD, Moreno-De-Luca D, Poultney CS, Robinson EB, Smith L, Solli-Nowlan T, Su MY, Teran NA, Walker MF, Werling DM, Beaudet AL, Cantor RM, Fombonne E, Geschwind DH, Grice DE, Lord C, Lowe JK, Mane SM, Martin DM, Morrow EM, Talkowski ME, Sutcliffe JS, Walsh CA, Yu TW, Autism Sequencing Consortium, Ledbetter DH, Martin CL, Cook EH, Buxbaum JD, Daly MJ, Devlin B, Roeder K, State MW (2015) Insights into autism spectrum disorder genomic architecture and biology from 71 risk loci. Neuron 87:1215–1233. https://doi.org/10.1016/j.neuron.2015.09.016

Sebat J, Lakshmi B, Malhotra D, Troge J, Lese-Martin C, Walsh T, Yamrom B, Yoon S, Krasnitz A, Kendall J, Leotta A, Pai D, Zhang R, Lee Y-H, Hicks J, Spence SJ, Lee AT, Puura K, Lehtimäki T, Ledbetter D, Gregersen PK, Bregman J, Sutcliffe JS, Jobanputra V, Chung W, Warburton D, King M-C, Skuse D, Geschwind DH, Gilliam TC, Ye K, Wigler M (2007) Strong association of de novo copy number mutations with autism. Science 316:445–449. https://doi.org/10.1126/science.1138659

Shaw KA, Williams S, Patrick ME, Valencia-Prado M, Durkin MS, Howerton EM, Ladd-Acosta CM, Pas ET, Bakian AV, Bartholomew P, Nieves-Muñoz N, Sidwell K, Alford A, Bilder DA, DiRienzo M, Fitzgerald RT, Furnier SM, Hudson AE, Pokoski OM, Shea L, Tinker SC, Warren Z, Zahorodny W, Agosto-Rosa H, Anbar J, Chavez KY, Esler A, Forkner A, Grzybowski A, Agib AH, Hallas L, Lopez M, Magaña S, Nguyen RHN, Parker J, Pierce K, Protho T, Torres H, Vanegas SB, Vehorn A, Zhang M, Andrews J, Greer F, Hall-Lande J, McArthur D, Mitamura M, Montes AJ, Pettygrove S, Shenouda J, Skowyra C, Washington A, Maenner MJ (2025) Prevalence and Early Identification of

Autism Spectrum Disorder Among Children Aged 4 and 8 Years - Autism and Developmental Disabilities Monitoring Network, 16 Sites, United States, 2022. MMWR Surveill Summ 74:1–22. https://doi.org/10.15585/mmwr.ss7402a1

Sohal VS, Rubenstein JLR (2019) Excitation-inhibition balance as a framework for investigating mechanisms in neuropsychiatric disorders. Mol Psychiatry 24:1248–1257. https://doi.org/10.1038/s41380-019-0426-0

Sohal VS, Zhang F, Yizhar O, Deisseroth K (2009) Parvalbumin neurons and gamma rhythms enhance cortical circuit performance. Nature 459:698–702. https://doi.org/10.1038/nature07991

Sparrow SS, Cicchetti DV, Balla D (2005) Vineland Adaptive Behavior Scales, Second edition (Vineland-II). American Guidance Service, Circle Pines, MN

Sztainberg Y, Zoghbi HY (2016) Lessons learned from studying syndromic autism spectrum disorders. Nat Neurosci 19:1408–1417. https://doi.org/10.1038/nn.4420

Tang X, Jaenisch R, Sur M (2021) The role of GABAergic signalling in neurodevelopmental disorders. Nat Rev Neurosci 22:290–307. https://doi.org/10.1038/s41583-021-00443-x

Walsh T, McClellan JM, McCarthy SE, Addington AM, Pierce SB, Cooper GM, Nord AS, Kusenda M, Malhotra D, Bhandari A, Stray SM, Rippey CF, Roccanova P, Makarov V, Lakshmi B, Findling RL, Sikich L, Stromberg T, Merriman B, Gogtay N, Butler P, Eckstrand K, Noory L, Gochman P, Long R, Chen Z, Davis S, Baker C, Eichler EE, Meltzer PS, Nelson SF, Singleton AB, Lee MK, Rapoport JL, King M-C, Sebat J (2008) Rare Structural Variants Disrupt Multiple Genes in Neurodevelopmental Pathways in Schizophrenia. Science 320:539–543. https://doi.org/10.1126/science.1155174

Webb SJ, Naples AJ, Levin AR, Hellemann G, Borland H, Benton J, Carlos C, McAllister T, Santhosh M, Seow H, Atyabi A, Bernier R, Chawarska K, Dawson G, Dziura J, Faja S, Jeste S, Murias M, Nelson CA, Sabatos-DeVito M, Senturk D, Shic F, Sugar CA, McPartland JC (2023) The Autism Biomarkers Consortium for Clinical Trials: Initial Evaluation of a Battery of Candidate EEG Biomarkers. Am J Psychiatry 180:41–49. https://doi.org/10.1176/appi.ajp.21050485

Wickham H (2016) ggplot 2: Elegant Graphics for Data Analysis. Springer-Verlag, New York

Wilkinson CL, Nelson CA (2021) Increased aperiodic gamma power in young boys with Fragile X Syndrome is associated with better language ability. Mol Autism 12:17. https://doi.org/10.1186/s13229-021-00425-x

Wilkinson CL, Yankowitz LD, Chao JY, Gutiérrez R, Rhoades JL, Shinnar S, Purdon PL, Nelson CA (2024) Developmental trajectories of EEG aperiodic and periodic components in children 2–44 months of age. Nat Commun 15:5788. https://doi.org/10.1038/s41467-024-50204-4

Yizhar O, Fenno LE, Prigge M, Schneider F, Davidson TJ, O'Shea DJ, Sohal VS, Goshen I, Finkelstein J, Paz JT, Stehfest K, Fudim R, Ramakrishnan C, Huguenard JR, Hegemann P, Deisseroth K (2011) Neocortical excitation/inhibition balance in information processing and social dysfunction. Nature 477:171–178. https://doi.org/10.1038/nature10360

Authors and Affiliations

Vardan Arutiunian[1] · Catherine A. W. Sullivan[6] · Megha Santhosh[1] · Emily Neuhaus[1,2,3] · Heather Borland[1] · Raphael A. Bernier[2] · Susan Y. Bookheimer[4,5] · Mirella Dapretto[4,5] · Allison Jack[9] · Shafali Jeste[10] · James C. McPartland[7] · Adam Naples[7] · John D. Van Horn[11,12] · Kevin A. Pelphrey[13] · Sara Jane Webb[1,2,3] · Abha R. Gupta[6,7,8]

✉ Vardan Arutiunian
vardan.arutyunyan89@gmail.com

✉ Sara Jane Webb
sara.webb@seattlechildrens.org

[1] Center for Child Health, Behavior and Development, Seattle Children's Research Institute, 1920 Terry Ave., Seattle, WA 98101, USA

[2] Department of Psychiatry and Behavioral Science, University of Washington, Seattle, WA, USA

[3] Institute on Human Development and Disability, University of Washington, Seattle, WA, USA

[4] Center for Autism Research and Treatment, Semel Institute for Neuroscience and Human Behavior, David Geffen School of Medicine, University of California Los Angeles, Los Angeles, CA, USA

[5] Department of Psychiatry and Biobehavioral Sciences, Semel Institute for Neuroscience and Human Behavior, David Geffen School of Medicine, University of California Los Angeles, Los Angeles, CA, USA

[6] Department of Pediatrics, Yale School of Medicine, Yale University, New Haven, CT, USA

[7] Yale Child Study Center, Yale School of Medicine, Yale University, New Haven, CT, USA

[8] Department of Neuroscience, Yale School of Medicine, Yale University, New Haven, CT, USA

[9] Department of Psychology, George Mason University, Fairfax, VA, USA

[10] Department of Pediatrics and Neurology, USC Keck School of Medicine, Children's Hospital of Los Angeles, Los Angeles, CA, USA

[11] School of Data Science, University of Virginia, Charlottesville, VA, USA

[12] Department of Psychology, University of Virginia, Charlottesville, VA, USA

[13] Department of Neurology, School of Medicine, University of Virginia, Charlottesville, VA, USA